Science Front Publishers *Journal for Foundations and Applications of Physics*, **vol. 8, No. 1 (2021)**
(sciencefront.org) **ISSN 2394-3688**

The Effect of Varying Soot Concentration and Relative Humidity on Visibility and Particle Size Distribution in Urban Atmosphere

Abdulkarim U. Y.[1*], Yerima S. U. [2], Tijjani B. I.[3], Gana U. M. [3] and Sani M. [4]

[1] Department of Physics, Saadatu Rimi College of Education Kano, Kano State Nigeria.
[2] Nigerian Meteorological Agency (NIMET), Nnamdi Azikwe International Airport Abuja.
[3] Department of Physics, Bayero University Kano, Kano State Nigeria.
[4] Centre for Atmospheric Research, National Space Research and Development Agency (NASRDA) Anyigba, Kogi State Nigeria.
**Corresponding Author*: gjummu.physicist@yahoo.com

(Received 05 March 2021, Accepted 11 April 2021, Published 29 April 2021)

Abstract

This research used extracted extinction coefficients and common mode radii of urban aerosols to carry out visibility simulations at corresponding spectral wavelengths from 0.4-0.8μm from the improved version of the Optical Properties of Aerosols and Clouds (OPAC 4.0) data at eight relative humidities (RH) (0%, 50%, 70%, 80%, 90%, 95%, 98% and 99% RH). Five models of the urban aerosols used comprised of insoluble (INSO), Water-soluble (WASO) and Soot (Black Carbon). From the average concentration set up by OPAC 4.0, the concentrations of the Soot (Black Carbon) were varied by external mixing. The Angstrom exponent (α), the curvature (α_2) and the urban atmospheric turbidity (β) were obtained from the regression analysis of the first and second order polynomial of Kaufman's representation of the Koschmieder equation for atmospheric visibility. The mean exponents of the aerosol size growth curve (μ) were determined from the aerosol effective hygroscopic growth (g_{eff}) while the humidification factors (γ) were determined from the visibility enhancement factors f(RH,λ). With μ and γ, the mean exponents of aerosol size distributions (υ) were determined for all the models. It was observed that at varying Soot (Black Carbon) concentrations and RH there were non-linear relationships between them and visibilities. The values of $\alpha > 1$ showed the presence of fine mode particles from the WASO part of the aerosol mixture and α_2 being positive indicated bimodal aerosol particle distributions. Additionally, visibility deterioration is predicted because of the increase in turbidity (β) with the variation of Soot and RH.

***Keywords*:** Aerosol Size Distribution, Humidification Factor, Hygroscopicity, Soot

1. Introduction

Soot also known as black carbon comes primarily from the incomplete combustion of fossil fuel and biomass burning. Most black carbon particles in the atmosphere are from man-made activities [1-3]. The emission of black carbon particles into the atmosphere varies from region to region all depending on fossil fuel usage, rapid urbanization and technological development mostly found in developing countries [1, 4].

Soot (BC) has become one of the carbonaceous aerosols gaining considerable significance in the atmospheric sciences because of its radiative and climatic impact as it can absorb sunlight, impact regional circulation and rainfall patterns unlike other aerosol types like sulfates [5-7]. Soot has been determined to be the second strongest contributor to global warming next to carbon dioxide [1, 8-10]. Soot particles are hydrophobic and are the largest absorbers of radiation in the atmosphere in both the shortwave and long wave region.

One contributing factor for the inability of current climate models to accurately estimate surface visibilities is due to the inaccurate characterization of soot (BC) concentration and particle size distribution effects. Therefore it is important to provide adequate validative information on the spatial and varying concentration effects. This will help towards predicting realistic global estimates of aerosol radiative effects more confidently [9-12].

In this paper an analysis was carried out on the effects of varying soot (BC) aerosol particle concentration and relative humidity on visibility and particle size distribution in urban atmosphere using simulation methods. This information is crucial in environmental quality assessment [13-27]. The extinction coefficients were extracted to determine visibilities and visibility enhancement factors while aerosol particle radii were extracted to determine the effective hygroscopic growth to simulate the impact of relative humidity (RH) on visibility in urban atmosphere which comprise of soot, water-soluble and insoluble aerosol components at different concentrations from OPAC 4.0.The concentrations of SOOT (BC) aerosol component were varied through external mixing to analyze their effect on both visibility, effective hygroscopic growth and particle size distribution.

2.0 Methodology

The models presented in Table 1 were used for the simulations of the aerosol components.

Table 1: Five model component mixtures with varying SOOT aerosol concentration

	Model 1	Model 2	Model 3	Model 4	Model 5
Comp	Number Density (cm^{-3})	Number Density (cm^{-3})	Number Density (cm^{-3})	Number Density (cm^{-3})	Number Density (cm^{-3})
Inso	1.50	1.50	1.50	1.50	1.50
Waso	28,000.00	28,000.00	28,000.00	28,000.00	28,000.00
Soot	**132,000.00**	**134,000.00**	**136,000.00**	**138,000.00**	**140,000.00**

2.1 Visibility and Relative Humidity

For visibility simulations, extinction coefficients were extracted for each relative humidity (RH) at corresponding visible spectral wavelength. The visibility was calculated based on the Koschmieder formula [28].

$$V_{Vis}(\lambda) = \frac{3.912}{\sigma_{ext}(\lambda)} \quad (1)$$

But the extinction coefficient is defined in terms of wavelength using inverse power law as [29];

$$\sigma_{ext}(\lambda) = \beta\lambda^{-\alpha} \quad (2)$$

Therefore substituting Eq. (2) into Eq. (1) gives;

$$V_{Vis}(\lambda) = \frac{3.912}{\beta}\lambda^{\alpha} \quad (3)$$

According to [30] Eq. (3) can be expressed as;

$$\ln\left(\frac{V_{Vis}(\lambda)}{3.912}\right) = \alpha\ln(\lambda) - \ln(\beta) \quad (4)$$

To obtain α (Angstrom exponent) and β (turbidity) a regression analysis was performed using an expression derived from the [31] representation of Eq. (1) [28]. However the Angstrom exponent itself varies with wavelength and an empirical relationship between visibility and wavelength is obtained with a 2nd-order polynomial [32-34]

$$\ln\left(\frac{V_{Vis}(\lambda)}{3.912}\right) = \alpha_1(\ln(\lambda)) + \alpha_2(\ln(\lambda))^2 - \ln(\beta) \quad (5)$$

The coefficient α_2 accounts for a “curvature” often observed in sun photometry measurements. The curvature depicts the aerosol particle size as indicated by [40]. Negative curvature indicates aerosol size distribution dominated by fine mode particles and positive curvature indicates size distribution dominated by coarse mode particles [31, 35].

.

2.2 Visibility Enhancement Factor

To determine the influence of relative humidity (RH) on the visibility enhancement factor f(RH,λ), the expression for visibility enhancement parameter f(RH,λ) given by [41] and [44] is applied as follows;

$$f(RH,\lambda) = \frac{V_{Vis}(RH,\lambda)}{V_{Vis}(RH_0,\lambda)} = \left[\frac{1-RH}{1-(RH_0)}\right]^{-\gamma} \quad (6)$$

Eq. (6) can also be written as;

$$ln\left(\frac{V_{Vis}(RH,\lambda)}{V_{Vis}(RH_0,\lambda)}\right) = -\gamma ln(1-RH) \quad (7)$$

where $RH_0 = 0\%$ and $V_{Vis}(RH,\lambda)$ is the visibility at wavelength λ at certain relative humidity (RH) such that the humidification factor γ can be expressed as [36];

$$\mu\gamma = \upsilon - 1 \tag{8}$$

where γ is the humidification factor that represents the dependence of visibility on relative humidity (RH) resulting from the change in the particle size and refractive indices of the aerosol particles upon humidification. γ also describes the hygroscopic behavior of visibility in a linear manner over a broad range of relative humidity values which also implies that particles are deliquesced [37] μ is the mean exponent of the aerosol growth curve [38]. υ is the mean exponent of the aerosol size distribution presented in the Junge power law size distribution function;

$$\frac{dn(r)}{d(logr)} = cr^{-\upsilon} \tag{9}$$

with c as a constant and $dn(r)$ representing number of particles with radii between r and $r + dr$. As υ value decreases, the number of larger particles increases compared to the number of smaller particles. For haze, υ takes value of about 3 and fogs have value of 2 [30].

2.3 Hygroscopic Growth

The hygroscopic growth$g(RH)$ experienced by a single particle according to [39] is given by;

$$g(RH) = \frac{r(RH)}{r(RH_0)} \tag{10}$$

with $r(RH)$ being the radius at a given relative humidity RH and $r(RH_0)$ representing the radius at 0% relative humidity.

But since atmospheric aerosols comprised of aerosols of different types and of different composition, Eq. (10) is replaced with the effective hygroscopic growth as;

$$g_{eff}(RH) = \left(\sum_k x_k g_k^3(RH)\right)^{\frac{1}{3}} \tag{11}$$

where x_k is the volume mix ratio of the k[th] term and r_k is particle radii of the k[th] component [37].

Expressing the effective hygroscopic growth in terms of relative humidity (RH) gives [39];

$$g_{eff}(RH) = \left[\frac{1-(RH)}{1-(RH_0)}\right]^{-\frac{1}{\mu}} \tag{12}$$

where μ is the mean exponent of the aerosol growth curve as defined in Eq. (8). Now taking the natural log of both sides of Eq. (11) gives;

$$lng_{eff}(RH) = -\frac{1}{\mu}ln(1 - RH) \tag{13}$$

Now expressing υ (the mean exponent of the aerosol size distribution) in terms of μ (the mean exponent of the aerosol growth curve) and γ (the humidification factor) using Eq. (8) and Eq. (11) gives the following;

$$\upsilon = \mu\gamma + 1 \quad (14)$$

3.0 Results and Discussions

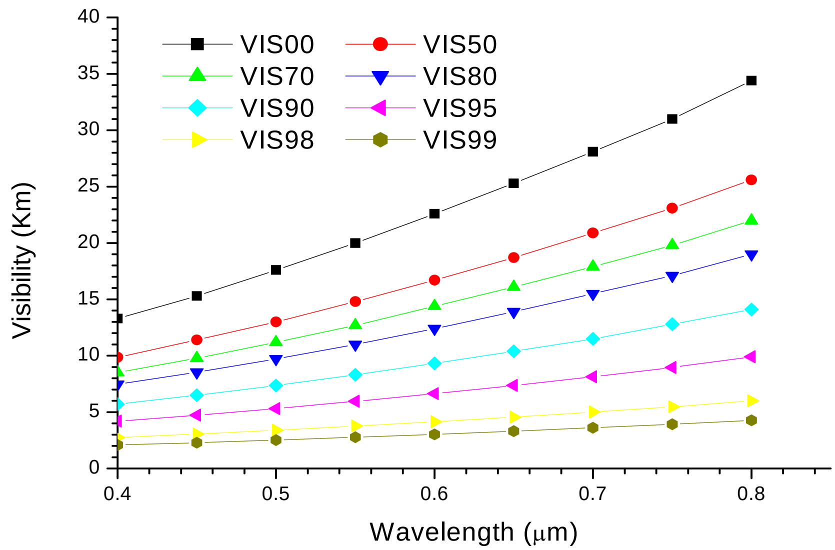

Fig. 1: Visibility against Wavelength for Table 1 Model 1

From Fig. 1, it can be seen that the visibility decreases with the increase in RH but increases with the increase in wavelength There is a more noticeable decrease in visibility with increase in relative humidity (RH) from 0% (RH) to 50% (RH) due to the onset of the intake of water by the absorbing black carbon

Table 2: Model 1 results of regression analysis of Eq. (4) and Eq. (5) for visibility using SPSS

	Linear			Quadratic			
RH	R^2	α	β	R^2	α_1	α_2	β
0%	0.99951	1.37274	0.08512	0.99998	1.61085	0.21116	0.08045
50%	0.99923	1.37875	0.11444	0.99998	1.68289	0.26972	0.10647
70%	0.99908	1.36960	0.13378	0.99998	1.70256	0.29528	0.12362
80%	0.99892	1.35364	0.15547	0.99998	1.71004	0.31606	0.14286
90%	0.99861	1.30913	0.21176	0.99999	1.70180	0.34823	0.19293
95%	0.99818	1.23963	0.30756	0.99999	1.66557	0.37774	0.27800
98%	0.99756	1.12319	0.52123	0.99999	1.57091	0.39705	0.46870
99%	0.99698	1.03651	0.74611	0.99999	1.49665	0.40807	0.66894

From Table 2, the R^2 values from both the quadratic and linear part shows that the data fitted the equation models very well. It can be seen from the linear part that the values of α are greater than 1, this shows dominance of soot (absorbing black carbon) particles. It can also be seen that α decreases with increase in relative humidity (RH) and this can be attributed to the hygroscopic growth of the aerosol as a result of the water uptake from the atmosphere. For the quadratic part, α_2 is positive for all relative humidities, indicating bimodal aerosol particle distribution.

Table 3: Model 1 analysis of Eq. (7), Eq. (12) and Eq. (13) using SPSS

			μ=5.12877
λ	R^2	γ	υ
0.55	0.99891	0.41642	3.13574
0.65	0.99857	0.42490	3.17921
0.75	0.99818	0.42942	3.20240

From Table 3, it can be seen that the humidification factor (γ) increases with the increase in λ. It can also be seen that for a given mean exponent hygroscopic growth curve (μ=5.12877) the mean exponent size distribution (υ) increases with the increase in wavelength (λ). This implies that apart from the dominance of fine mode particle, the aerosols comprise of coarse particles of different sizes. υ takes values > 3 which implies typical hazy conditions in the urban atmosphere [38].

Table 4: Skewness and Kurtosis Model 1

	Vis00	Vis50	Vis70	Vis80	Vis90	Vis95	Vis98	Vis99
Skewness	-0.22957	-0.17910	-0.17195	-0.17889	-0.13801	-0.12102	-0.08945	-0.06484
Kurtosis	-1.12855	-1.11494	- 1.13305	-1.16736	-1.14481	-1.17458	-1.18633	-1.20311

From Table 4, the changes of the particles distribution are displayed in terms of horizontal behavior (skewness) and vertical behavior (Kurtosis). The skewness at visibility 0% to 99%RH is negative. This behavior in terms of aerosols particle size distribution can be said to be dominated by coarse mode particles. It can be seen that from 0% to 99%RH, there is an increase in skewness which implies an increase in particle size distribution which may be due to the addition of soot into the atmosphere from active sources. For kurtosis it can be seen that they are all negative and this shows that the size distribution of the particles is platykurtic. As from 0% to 99%RH, there are a lot of fluctuations this may also be attributed to the non linear relationship of the physically mixed aerosols with relative humidity (RH).

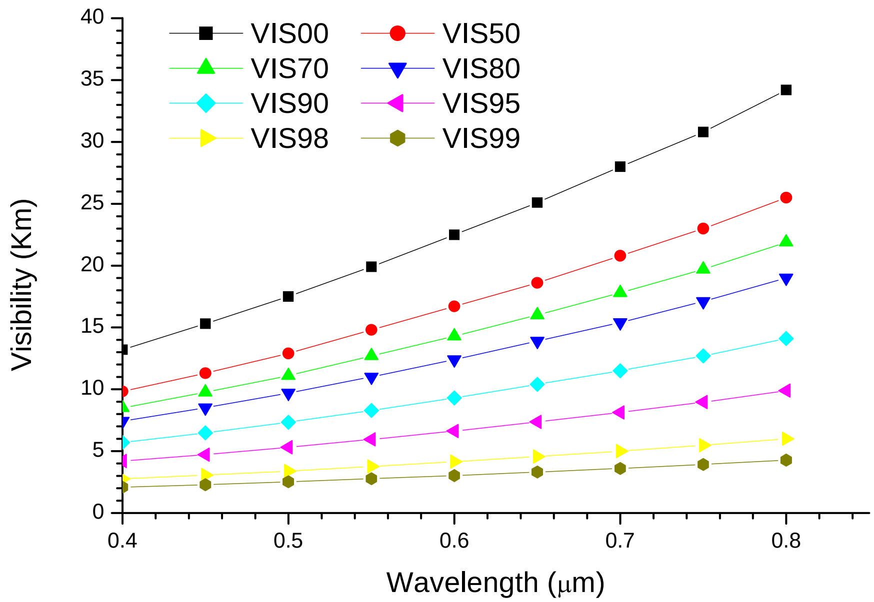

Fig. 2: Visibility against Wavelength for Table 1 Model 2

From Fig. 2, the visibility decreases with the increase in RH but increases with the increase in wavelength. Visibility is lower at shorter wavelength due to dominance of soot particles.

Table 5: Model 2 results of regression analysis of Eq. (4) and Eq. (5) for visibility using SPSS

	Linear			Quadratic			
RH	R^2	α	β	R^2	$α_1$	$α_2$	β
0%	0.99951	1.37312	0.08559	0.99998	1.61254	0.21232	0.08086
50%	0.99923	1.37924	0.11489	0.99998	1.68380	0.27009	0.10688
70%	0.99909	1.36977	0.13426	0.99998	1.69929	0.29223	0.12416
80%	0.99893	1.35383	0.15595	0.99998	1.70814	0.31421	0.14338
90%	0.99862	1.30937	0.21224	0.99999	1.70093	0.34724	0.19341
95%	0.99819	1.23973	0.30806	0.99999	1.66413	0.37637	0.27855
98%	0.99752	1.12314	0.52177	0.99999	1.57392	0.39977	0.46884
99%	0.99695	1.03668	0.74668	0.99999	1.49914	0.41012	0.66908

From Table 5, the R^2 values from both the quadratic and linear part shows that the data fitted the equation models very well. It can be seen from the linear part that the values of α are greater than 1, this shows dominance of soot (absorbing black carbon) particles. It can also be seen that α decreases with increase in relative humidity (RH) and this can be attributed to the hygroscopic growth of the aerosol as a result of the water uptake from the atmosphere by the soluble coating of the soot particles. For the quadratic part, $α_2$ is positive for all relative humidities, indicating bimodal aerosol particle distribution.

Table 6: Model 2 analysis of Eq. (7), Eq. (12) and Eq. (13) using SPSS

			μ=5.13031
λ	R^2	γ	υ
0.55	0.99888	0.41520	3.13009
0.65	0.99854	0.42363	3.17336
0.75	0.99815	0.42822	3.19688

From Model 2, the values of R^2 show that the model equation fits the data very well. From observation, the humidification factor (γ) increases with the increase in λ. This implies that the aerosols comprise of both fine mode particles and coarse mode particles of different sizes. For a given mean exponent hygroscopic growth curve (μ= 5.13031) it can be seen that the mean exponent size distribution (υ) increases with the increase in wavelength (λ). υ takes values > 3 which implies typical hazy conditions in the urban atmosphere [38].

Table 7: Skewness and Kurtosis Model 2

	Vis00	Vis50	Vis70	Vis80	Vis90	Vis95	Vis98	Vis99
Skewness	-0.21545	-0.18966	-0.19904	-0.15983	-0.14940	-0.12187	-0.08911	-0.06553
Kurtosis	-1.11958	-1.11814	-1.14395	-1.15634	-1.16995	-1.17537	-1.18430	-1.20060

From Table 7, the skewness at all relative humidities is negative. This is an indication of aerosol particle size distribution dominated by coarse soot particles. The changes of the particles distribution are displayed in terms of horizontal behavior (skewness) and vertical behavior (Kurtosis). The skewness increases from 0% to 95%RH which implies an increase of particle size distribution. For kurtosis it can be seen that they are all negative and this shows platykurtic distribution.

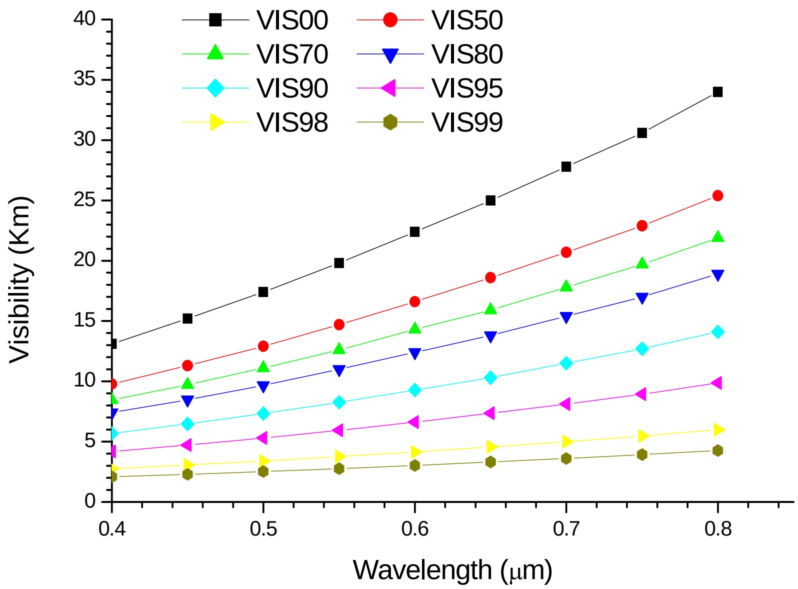

Fig. 3: Visibility against Wavelength for Table 1 Model 3

From Fig. 3, the visibility decreases with increase in RH but increases with increase in wavelength. There is a more noticeable decrease in visibility with increase in relative humidity (RH) from 0% (RH) to 50% (RH) due to the onset of the intake of water by aerosol particles.

Table 8: Model 3 results of regression analysis of Eq. (4) and Eq. (5) for visibility using SPSS

	Linear			Quadratic			
RH	R^2	α	β	R^2	α_1	α_2	β
0%	0.99953	1.37293	0.08609	0.99997	1.60623	0.20689	0.08146
50%	0.99925	1.37893	0.11541	0.99998	1.67924	0.26632	0.10747
70%	0.99909	1.37007	0.13473	0.99998	1.70113	0.29359	0.12455
80%	0.99893	1.35419	0.15641	0.99998	1.70939	0.31500	0.14377
90%	0.99862	1.30982	0.21269	0.99999	1.70011	0.34612	0.19387
95%	0.99820	1.24025	0.30849	0.99999	1.66407	0.37585	0.27898
98%	0.99755	1.12371	0.52219	0.99999	1.57196	0.39752	0.46950
99%	0.99696	1.03681	0.74720	0.99999	1.49827	0.40923	0.66971

From Table 8 Model 3, the R^2 values from both the quadratic and linear part shows that the data fitted the equation models very well. It can be seen from the linear part that the values of α are greater than 1, this shows the presence dominance of soot particles. It can also be seen that α decreases with increase in relative humidity (RH) and this can be attributed to the hygroscopic growth of the soluble aerosols physically mixed with the soot particles within the atmosphere. α_2 is positive for all relative humidities, indicating bimodal aerosol particle distribution.

Table 9: Model 3 analysis of Eq. (7), Eq. (12) and Eq. (13) using SPSS

			μ=5.13170
λ	R^2	γ	υ
0.55	0.99886	0.41399	3.12447
0.65	0.99851	0.42238	3.16752
0.75	0.99810	0.42678	3.19011

From Table 9, for a given mean exponent hygroscopic growth curve (μ= 5.13170) it can be seen that the mean exponent size distribution (υ) increases with the increase in wavelength (λ). By observing the humidification factor (γ) it also increases with the increase in λ, this implies the dominance of fine mode particles from the soluble part of the mixture taking up water. υ takes values > 3 which implies typical hazy conditions in the urban atmosphere [38].

Table 10: Skewness and Kurtosis Model 3

	Vis00	Vis50	Vis70	Vis80	Vis90	Vis95	Vis98	Vis99
Skewness	-0.20716	-0.18254	-0.16558	-0.15441	-0.14679	-0.12109	-0.08944	-0.06489
Kurtosis	-1.11402	-1.17165	-1.14031	-1.14348	-1.17405	-1.17332	-1.18611	-1.19507

From Table 10 model 3, skewness is negative at all relative humidities. This implies that the aerosol particle size distribution is dominated by coarse mode particles. From 0% to 99%RH the skewness is increasing and this implies an increased particle size distribution. The negative kurtosis implies a platykurtic distribution. There are fluctuations from 0% to 99%RH which may also be attributed to the non linear relation of the physically mixed aerosols with relative humidity (RH).

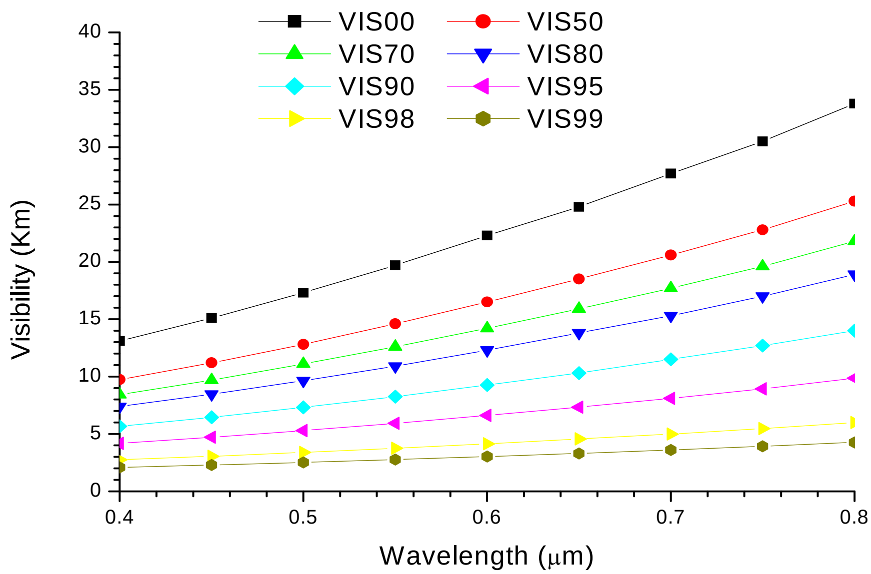

Fig. 4: Visibility against Wavelength for Table 1 Model 4

From Fig. 4, it can be seen that the visibility decreases with the increase in RH but increases with the increase in wavelength. There is a more noticeable decrease in visibility with increase in relative humidity (RH) from 0% (RH) to 50% (RH) due to the onset of the intake of water by the water soluble part of the aerosol mixture.

Table 11: Model 4 results of regression analysis of Eq. (4) and Eq. (5) for visibility using SPSS

	Linear			Quadratic			
RH	R^2	α	β	R^2	α_1	α_2	β
0%	0.99954	1.37286	0.08659	0.99997	1.60476	0.20565	0.08195
50%	0.99925	1.37914	0.11587	0.99998	1.68096	0.26767	0.10787
70%	0.99909	1.36989	0.13523	0.99998	1.69977	0.29255	0.12505
80%	0.99894	1.35399	0.15692	0.99998	1.70756	0.31355	0.14429
90%	0.99863	1.30994	0.21318	0.99999	1.69927	0.34527	0.19437
95%	0.99821	1.24034	0.30902	0.99999	1.66301	0.37484	0.27953
98%	0.99758	1.12381	0.52269	0.99999	1.56979	0.39550	0.47021
99%	0.99698	1.03681	0.74779	0.99999	1.49663	0.40778	0.67050

From Table 11 Model 4, the R^2 values from both the quadratic and linear part shows that the data fitted the equation models very well. From the linear part, α values are greater than 1, this shows dominance of soot particles. It can also be seen that α decreases with increase in relative humidity (RH) and this can be attributed to the hygroscopic growth of the water soluble aerosols within the physically mixed aerosols. For the quadratic part α_2 is positive for all relative humidities, indicating bimodal aerosol particle distribution with dominance of fine mode particles.

Table 12: Model 4 analysis of Eq. (7), Eq. (12) and Eq. (13) using SPSS

			μ=5.13321
λ	R^2	γ	υ
0.55	0.99884	0.41278	3.11889
0.65	0.99847	0.42114	3.16182
0.75	0.99807	0.42561	3.18477

From Table 12, for a given mean exponent hygroscopic growth curve (μ= 5.13321) it can be seen that the mean exponent size distribution (υ) increases with the increase in wavelength (λ). The humidification factor (γ) also increases with the increase in λ, due to the presence of water soluble aerosols within the soot aerosol mixture. υ takes values > 3 which implies typical hazy conditions in the urban atmosphere [38].

Table 13: Skewness and Kurtosis Model 4

	Vis00	Vis50	Vis70	Vis80	Vis90	Vis95	Vis98	Vis99
Skewness	-0.21545	-0.18776	-0.17417	-0.17931	-0.13745	-0.12227	-0.08958	-0.06433
Kurtosis	-1.11958	-1.12172	-1.13120	-1.16269	-1.15211	-1.17239	-1.18589	-1.19508

From Table 13 skewness is negative at all relative humidities and it can be said that the particle size distribution is dominated by coarse mode soot particles. As from 0% to 99%RH the skewness is increasing and this implies an increase in particle size distribution. For kurtosis it can be seen that they are all negative and this shows a platykurtic particle size distribution. As from 0% to 99%RH, there are a lot of fluctuations this may also be attributed to the non linear relation of the physically mixed aerosols with relative humidity (RH).

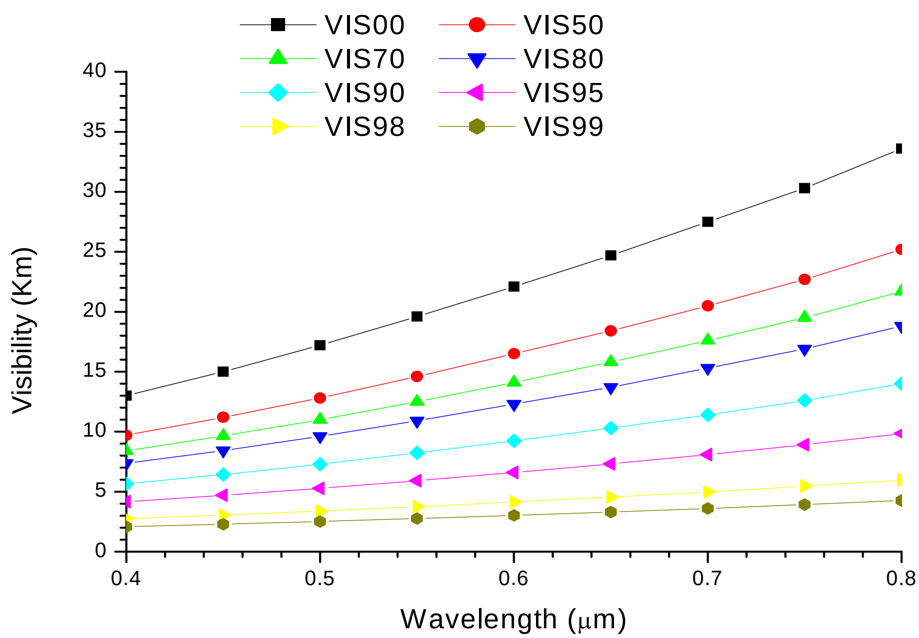

Fig. 5: Visibility against Wavelength for Table 1 Model 5

From Fig. 5, the visibility decreases with the increase in RH but increases with the increase in wavelength. The onset of the intake of water by aerosol particles shows a more noticeable decrease in visibility with increase in relative humidity (RH) from 0% (RH) to 50% (RH). This shows evidence of the presence of water soluble aerosols within the mixture.

Table 14: Model 5 results of regression analysis of Eq. (4) and Eq. (5) for visibility using SPSS

	Linear			Quadratic			
RH	R^2	α	β	R^2	α_1	α_2	β
0%	0.9995	1.3736	0.0870	0.9999	1.6062	0.2062	0.08235
50%	0.9992	1.3791	0.1163	0.9999	1.6795	0.2663	0.10836
70%	0.9991	1.3696	0.1357	0.9999	1.6966	0.2899	0.12561
80%	0.9989	1.3544	0.1573	0.9999	1.7081	0.3136	0.14470
90%	0.9986	1.3102	0.2136	0.9999	1.6996	0.3453	0.19478
95%	0.9982	1.2407	0.3094	0.9999	1.6637	0.3751	0.27992
98%	0.9975	1.1241	0.5231	0.9999	1.5735	0.3985	0.47026
99%	0.9969	1.0373	0.7481	0.9999	1.5003	0.4106	0.67032

From Table 14 Model 5, the R^2 values show that the data fitted the equation models very well. It can be seen from the linear part that the values of α are greater than 1, this shows dominance of soot particles. It can also be seen that α decreases with increase in relative humidity (RH) and this can be attributed to the hygroscopic growth of the water soluble part of the aerosol mixture. For the quadratic part α_2 is positive for all relative humidities, indicating bimodal aerosol particle distribution.

Table 15: Model 5 analysis of Eq. (7), Eq. (12) and Eq. (13) using SPSS

			μ=5.13466
λ	R^2	γ	υ
0.55	0.99881	0.41165	3.11369
0.65	0.99845	0.42009	3.15700
0.75	0.99804	0.42445	3.17938

From Table 15, for a given mean exponent hygroscopic growth curve (μ= 5.13466) it can be seen that the mean exponent size distribution (υ) increases with the increase in wavelength (λ). By observing the humidification factor (γ) it also increases with the increase in λ because of the soluble part of the mixture. υ takes values > 3 which implies typical hazy conditions in the urban atmosphere [38].

Table 16: Skewness and Kurtosis Model 5

	Vis00	Vis50	Vis70	Vis80	Vis90	Vis95	Vis98	Vis99
Skewness	-0.20972	-0.19356	-0.20124	-0.17210	-0.13838	-0.12096	-0.08866	-0.06377
Kurtosis	-1.13231	-1.17463	-1.14198	-1.13521	-1.14006	-1.17252	-1.18922	-1.19744

From Table 16, it can be seen that skewness is negative at 0% to 99%RH. This behavior in terms of aerosol particle size distribution can be said to be dominated by coarse mode particles. For kurtosis it can be seen that they are all negative and this shows that the size distribution of the particles is platykurtic. At all relative humidities, there are a lot of fluctuations this may also be attributed to the non linear relation of the physically mixed aerosols with relative humidity (RH).

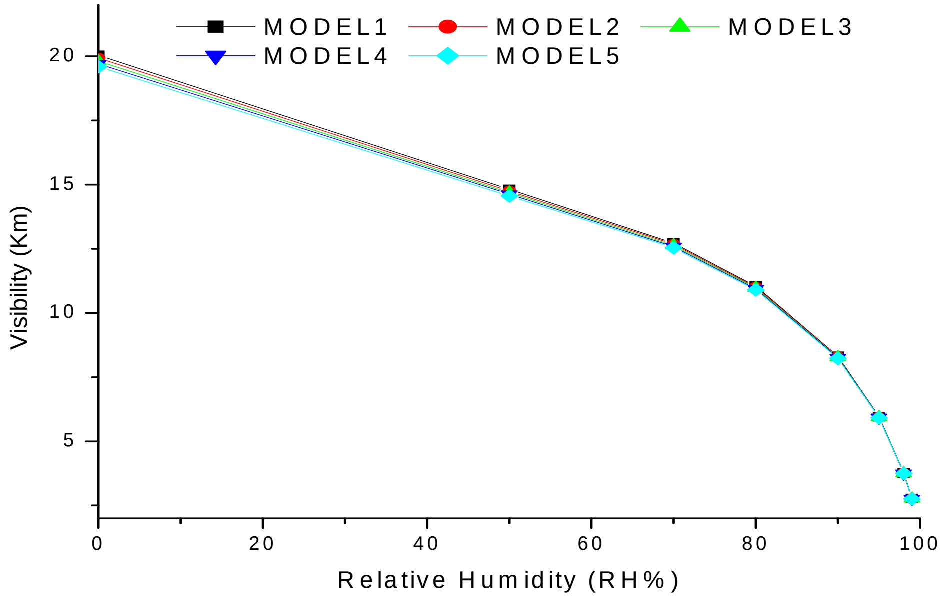

Fig. 6: Graph of Visibility (Km) against Relative Humidity (RH%) at varying SOOT concentration

Fig 6. Is a graph of visibility against relative humidity at the green visible spectral wavelength of 0.55μm showing how visibility changes at varying SOOT concentration for the five models. The graph shows that as SOOT concentration increases, visibility decreases at rising relative humidity (RH).

4. Summary and Conclusion

From all the five models considered it was observed that:

(1) Across all the models, α values were greater than 1 and the values increased with the increase in RH as SOOT concentrations increased.

(2) α_2 showed that the mode radii of all particles were bimodal and they fluctuated across the models with increase in SOOT concentration and RH.

(3) Visibilities decreased with the increase in SOOT concentrations and RH across all the models.

(4) The skewness was negative for all the models and increased and the kurtosis was negative across all the models and fluctuated in magnitude.

(5) Across the models, the mean exponent hygroscopic growth curve (μ) increased with increase in SOOT concentration.

(6) The mean exponent size distributions (υ) increased with the increase in wavelength (λ) for each of the models but decreased with increase in SOOT concentration across all the models.

(7) The humidification factors (γ) increased with the increase in wavelength (λ) for each of the models but decreased with increase in SOOT concentration across all the models.

The presence of coarse mode particles due to soot emissions in urban atmosphere has been established with the values of the Angstrom exponent (α), the curvature (α_2), skewness and kurtosis at varying SOOT concentrations. It can be concluded that visibility decreases with an increase in relative humidity and SOOT aerosol concentration. The values of α greater than 1, implies the presence of soot particles and the presence of fine mode particles from the water soluble part of the atmospheric aerosol mixture. α_2 fluctuates as a result of the changes in RH and particle concentration which may be attributed to the non-linear relationship between physically mixed aerosols with relative humidity (RH) as soot concentration increases. As the SOOT concentration increased across the models, μ increased and this implies that there is a direct relationship between them. The increase in the values of υ with the increase in λ implies a direct relationship between them and this showed that the increase in SOOT caused an increase particle size distribution. The increase in γ values with increase in λ also shows a direct relationship that indicates increase in aerosol particle hygroscopicity due to the water soluble part of the mixture. This could also be due to some type of porosity. Any hole within the black carbon particles may absorb part of the water at the beginning of the growth. The increase in the skewness indicates the presence of coarse mode soot particles and the fluctuations in the kurtosis signifies the non-linear relation of the physically mixed aerosols with relative humidity (RH) and water soluble aerosol concentration. The sign of kurtosis being negative shows that the particle size distributions are platykurtic.

References

[1] Ramachandran, S., and S. Kedia (2010), Black carbon aerosols over an urban region: Radiative forcing and climate impact, J. Geophys. Res., 115, D10202, doi:10.1029/2009JD013560.

[2] Chillrud, S.N., Bopp, R.F., Simpson, H.J., Ross, J.M., Shuster, E.L., Chaky, D.A., Walsh, D.C., Choy, C.C., Tolley, L.R., Yarme, A., 1999. Twentieth century atmospheric metal fluxes into Central Park Lake, New York City. Environmental Science and Technology 33, 657–662.

[3] Davis, A.P., Shokouhian, M., Ni, S., (2001). Loading estimates of lead, copper, cadmium, and zinc in urban runoff from specific sources. Chemosphere 44, 997–1009.

[4] Novakov, T., V. Ramanathan, J. E. Hansen, T. W. Kirchstetter, M. Sato, J. E. Sinton, and J. A. Sathaye (2003), Large historical changes of fossil- fuel black carbon aerosols, Geophys. Res. Lett., 30(6), 1324, doi:10.1029/2002GL016345.

[5] Morselli, L., Barilli, L., Olivieri, P., Cecchini, M., Aromolo, R., Di Carlo, V., Francaviglia, R., Gataleta, L., (1999a). Heavy metals determination in dry surrogate depositions. Characterisation of an urban and natural site. Annali di Chimica-Rome 89, 739–746.

[6] Morselli, L., Passarini, F., Zamagni, E., Brusori, B., (2000). Methodo-logical approach for an integrated environmental monitoring system relative to heavy metals from an incineration plant. Annali di Chi-mica - Rome 90, 723–732.

[7] Cabon, J.Y., (1999). Chemical characteristics of precipitation at an Atlantic station. Water, Air, and Soil Pollution 111, 399–416.

[8] Ramanathan, V., and G. Carmichael (2008), Global and regional climate changes due to black carbon, Nat. Geosci., 1, 221–227.

[9] Badarinath, K V S Latha, K Madhavi (2006). Direct radiative forcing from black carbon aerosols over urban environment . Advances in Space Research 37, 2183–218837

[10] D., Wu, X. X., Li, C. C., Ying, Z. M., Lau, A. K. H., Huang, J., X. J.,Deng, & X. Y. Bi, (2005): An extremely low visibility event over the Guangzhou region: A case study, *Atmos. Environ.*, 39(35), 6568–6577,

[11] A. S., Bret, B. H., Rudolf, R. F, Stefan. & E.W.,William (2001). Haze trends over the United States, 1980–1995. *Journal of Atmosphere and Environment*. 35: 5205–5210.

[12] Y.C., Chan, R.W., Simpson, G. H., Mctainsh, P. D., Vowles, D. D.,Cohen & G. M., Bailey, (1999). Source Apportionment of Visibility Degradation Problems in Brisbane (Australia) Using the Multiple Linear Regression Techniques. *Journal of Atmosphere and Environment*. 33: 3237–3250.

[13] M. Doylem & S., Dorling (2002). Visibility Trends in the UK 1950-1997. *Journal of Atmosphere and Environment*. 36: 3163–3172.

[14] R. A., Kotchenruther, P.V., Hobbs, D. A., Hegg, (1999). Humidification factors for atmospheric aerosol off the mid-Atlantic coast of United States. *J. Geophys. Res.* 104 (D2), 2239-2251.

[15] S.C., Yoon, J., Kim, (2006). Influences of relative humidity on aerosol optical properties and aerosol radiative forcing during ACE-Asia. *Atmos. Environ.* 40 (23), 4328-4338

[16] C. K., Chan, & X. H., Yao, (2008): Air pollution in mega cities in China, Atmos. Environ., 42, 1–42.

[17] X. J., Deng, X. X.,Tie D.,Wu, X. J., Zhou, X.Y., Bi, H. B.,Tan F., Li & C. L.,Jiang (2008): Long-Term Trend of Visibility and Its Characterizations in the Pearl River Delta (PRD) Region, China. *Journal of Atmosphere and Environment* .42(7), 1424–1435.

[18] P., Massoli, T.S., Bates, P.K., Quinn, D.A., Lack, T., Baynard, B.M., Lerner, S.C., Tucker, J., Brioude, A., Stohl, E.J.,Williams,(2009). Aerosol optical and hygroscopic properties during TexAQS-GoMACCS 2006 and their impact on aerosol direct radiative forcing. *J. Geophys. Res.* 114, D00F07.

[19] B. I. Tijjani (2013). The Effect of Soot and Water Soluble on the Hygroscopicity of Urban Aerosols. *Advances in Physics Theories and Applications* www.iiste.org ISSN 2224-719X (Paper) ISSN 2225-0638 (Online) Vol.26,

[20] Y. F.,Cheng, A.,Wiedensohler H.,Eichler J.,Heintzenberg M.,Tesche A.,Ansmann M.,Wendisch H.,Su Althausen D. H.,Herrmann T.,Gnauk E.,Bruggemann M., Hu Y.H.,Zhang (2008). Relative Humidity Dependence of Aerosol Optical Properties and Direct Radiative Forcing in The Surface Boundary Layer at Xinken in Pearl River Delta of China: An Observation Based Numerical Study. *Journal of Atmosphere and Environment*. 42, 6373-6397.

[21] H., Koschmieder, (1972): Theorie der horizontalenSichtweite, BeiträgezurPhysik der freien Atmosphäre, Meteorol. Z.,12, 33–55,

[22] X. Liu et al. (2012). 'Aerosol Hygroscopicity and Its Impact on Atmospheric Visibility and Radiative Forcing in Guangzhou during the 2006 PRIDE-PRD Campaign'. *Atmospheric Environment* 60: 59–67.

[23] X.G.,Liu, Y.H.,Zhang, J.S.,Jung, J.W., Gu, Y.P., Li, S.,Guo, S.Y.,Chang, D.,Yue, P.,Lin, Y.J.,Kim, M.,Hu, L.M.,Zeng, T., Zhu, (2009). Research on aerosol hygroscopic properties by measurement and model during the 2006 CARE Beijing campaign. *J. Geophys. Res.* 114, D00G16.

[24] X.G.,Liu, Y.H.,Zhang, M.T.,Wen, J.L.,Wang, J.S.,Jung, S.Y.,Chang, M.,Hu, L.M.,Zeng, Y.J.,Kim, (2010).A closure study of aerosol hygroscopic growth factor during the 2006 PRD campaign. *Adv. Atmos. Sci.*.

[25] J.S.,Reid, A.,Jayaraman, J.T.,Kiehl, T.N.Krishnamurti, & D.Lubin, (1999). Physical, chemical and optical regional hazes dominated by smoke in Brazil. *Journal of Geophysical Research,* 103: 32059-32080.

[26] S. Sjogren, et al. (2007). 'Hygroscopic Growth and Water Uptake Kinetics of Two-Phase Aerosol Particles Consisting of Ammonium Sulfate , Adipic and Humic Acid Mixtures'. 38: 157–71.

[27] B.I.Tijjani, A. Aliyu, & F. Shaaibu (2014b). 'The Effect of Relative Humidity on Continental Average Aerosols'. *Open Journal of Applied Sciences*, 4, 399-423 (6)

[28] M.King, & D. Byrne, (1976). A method for inferring total ozone content from the spectral variation of total optical depth obtained with a solar radiometer. *Journal of Geophysical Research*, 33: 3251-3254

[29] A. Ångström (1961). Techniques of Determining the Turbidity. Tellus, 13(2): 214-223.

[30] G.S.M.,Galadanci, B.I.,Tijjani, A.I.,Abubakar, F. S.,Koki, I. D.,Adamu, A. M.,Nura, M.,Saleh, & S.Uba, (2015): The Effect of Kelvin Effect On The Equilibrium Effective Radii And Hygroscopic Growth of Atmospheric Aerosols. IISTE- *Journal of Natural Sciences Research,* Vol.5, No.22, 2015 p96-111.

[31] F. Kasten (1969). Visibility forecast in the phase of pre-condensation. *Tellus*, XXI, 5, 631–635.

[32] Y. Kaufman (1993). Aerosol optical thickness and path radiance. *Journal of Geophysical research* 98 (D2) 2677-2692.

[33] I.N.,Tang, H.R.,Munkelwitz, (1994). Water activities, densities, and refractive indices of aqueous sulfate and sodium nitrate droplets of atmospheric importance. *J. Geophys. Res.* 99 (D9), 18,801-18,808.

[34] B. I., Tijjani, F. Sha'aibu & A. Aliyu (2014a).The Effect of Relative Humidity on Maritime Polluted Aerosols. *International Journal of Pure and Applied Physics* Vol.2, No.1, Pp.9-36,

[35] A.,Moln´ar, E.,M´esz´aros, K., Imre, & A.R¨ull, (2008): Trends in visibility over Hungary between 1996 and 2002, Atmos. Environ., 42, 2621–2629,

[36] B. I.,Tijjani, F.Sha'aibu & A. Aliyu. (2014a).The Effect of Relative Humidity on Maritime Polluted Aerosols. *International Journal of Pure and Applied Physics* Vol.2, No.1, Pp.9-36,

[37] P. K.,Quinn, et al. (2005) , Impact of particulate organic matter on the relative humidity dependence of light scattering: A simplified parameterization, Geophys. Res. Lett., 32, L22809,

[38] C. E. Junge, (1958). Atmospheric Chemistry. Advances in geophysics (Vol. 4, pp 1-108). Elsevier

[39] I. N.Tang (1996).Chemical and size effects of hygroscopic aerosols on light scattering coefficients. *Journal of Geophysical Research* 101 (D14), 19,245-19,250

[40] T. F.,Eck, B. N.,Holben, D. E., Ward,O., R. J. S.,Dubovic, A., Smirnov, M. M., Mukelabai N. C., Hsu, N. T.,O' Neil & I.Slutsker (2001) Characterization of The Optical Properties of Biomass Burning Aerosols in Zambia During the 1997 ZIBBEE Field Campaign, *Journal of Geophysics Research,* 106(D4), 3425–3448.

[41] E. Frankenberger, (1967) Beitr. Phys. Atmos. 37, 183.

[42] C. S.,Yuan, C. G, Lee, J. C. Chang & C.Yuan (2005) Effects of Aerosol Species on Atmospheric Visibility in Kaohsiung City, Taiwan. *Journal of Air & Waste Management Association.* 55:1031–1041

[43] Y.H.,Zhang, M., Hu, L.J.,Zhong, A.,Wiedensohler, S.C.,Liu, M.O.,Andreae, W.,Wang, S.J.,Fan, (2008). Regional integrated experiments on air quality over Pearl River Delta 2004 (PRIDE-PRD2004): overview. Atmos. Environ. 42, 6157-6173.

[44] P.,Zieger, R., Fierz-Schmidhauser, L.,Poulain, T., Müller, W.,Birmili, G.,Spindler, A.,Wiedensohler, Baltensperger, U., & E.Weingartner, (2013): Effects of relative humidity on aerosol light scattering: results from different European sites, Atmos. Chem. Phys., 13, 10609–10631.

[45] K. N.,Liou, Y.,Takano & P.Yang (2013). 'Journal of Quantitative Spectroscopy & Radiative Transfer Intensity and Polarization of Dust Aerosols over Polarized Anisotropic Surfaces'. *Journal of Quantitative Spectroscopy and Radiative Transfer* 127: 149–57.

[46] C.,Grandey S.Benjamin & C.Wang (2019). Background Conditions Influence the Estimated Cloud Radiative Effects of Anthropogenic Aerosol Emissions From Different Source Regions. *Journal of Geophysical Research: Atmospheres* 124(4): 2276–95